Electronic Supplementary Material (ESI) for ChemComm.

Supplementary Information

Poly(naphthalene diimide) Vinylene: Solid State Red Emission and Semiconducting Property for Transistor

Xianfeng Liang, Luxi Tan,* Zitong Liu, Guanxin Zhang, Yanping Ma,* Lin Wang, Shayu Li,
Lichun Dong, Jing Li* and Wei Chen

Contents

1. General information

Chemicals were purchased form Alfa-Aesar, Sigma-Aldrich etc. and used without further purification. Gel permeation chromatography (GPC) analysis was performed on a Waters 1515 chromatograph at 35 ℃, polystyrene was used as the calibration standard and THF as eluent. ^{1}H NMR and spectrum was obtained on Bruker DMX-600 NMR Spectrometers using tetramethylsilane as internal standard. Elemental analysis was performed on a Carlo Erba model 1160 elemental analyzer. Thin films absorption spectra were measured with PE lambda 950 UV-Vis spectrophtometer. The PL efficiencies were obtained by HAMAMATSU Absolute PL Quantum Yield Spectrometer C11347 at the excitation wavelength of 516 nm and 534 nm for solution and thin film, respectively. Fluorescence lifetimes were measured by HAMAMATSU Compact Fluorescence Lifetime Spectrometer C11367. TGA-DTA measurements were carried out on a NETZSCH STA 449 F3 Jupiter® instruments under a dry nitrogen flow, heating from room temperature to 550 ℃, with a heating rate of 20 ℃/min. Cyclic voltammetric measurements were carried out in a conventional three-electrode cell using glassy carbon (GC) as working electrodes of 2 mm diameter, a platinum wire as counter electrode, n-Bu_4NPF_6 (0.1 M)/acetonitrile as supporting electrolyte, and an Ag/AgCl reference electrode on a computer-controlled CHI660E instruments at room temperature. Grazing-incident X-ray diffraction (GIXRD) measurements were performed at 8ID-E beam line at the Advanced Photon Source (APS), Argonne National Laboratory using X-ray with a wavelength of $\lambda = 1.6868$. The molecular structures of the compounds were optimized using the DFT method at the level of RB3LYP/6-311G++(d,p). All calculations were performed with the programs Gaussian 09.

2. OFET device fabrication

Bottom-gate/bottom-contact FETs were fabricated. A heavily doped n-type Si wafer and a layer of dry oxidized SiO_2 (300 nm, with roughness lower than 0.1 nm and capacitance of 11 nF cm^{-2}) were used as a gate electrode and gate dielectric layer, respectively. The drain-source (D-S) gold contacts were fabricated by photolithography. The substrates were first cleaned by sonication in acetone and water for 5.0 min and immersed in piranha solution (2:1 mixture of sulfuric acid and 30% hydrogen peroxide) for 20 min. This was followed by rinsing with deionized water and isopropyl alcohol for several times, and it was blow-dried with nitrogen. Then, the surface was modified with n-octadecyltrichlorosilane (OTS). After that, the substrates were cleaned in n-hexane, $CHCl_3$, and isopropyl alcohol. The films of PNV were fabricated by spin-coating with their $CHCl_3$ solutions (10.0 mg/mL) at 2000 rpm. The annealing process was carried out in vacuum for 1.0 hr at the certain temperatures.

The field-effect characteristics of the devices were measured with Keithley 4200 SCS semiconductor parameter analyzer under ambient conditions. The mobility of the OFETs in the saturation region was extracted from the following equation:

$$I_{DS} = \frac{W}{2L}\mu C_i \left(V_{GS} - V_{th}\right)^2$$

where I_{DS} is the drain electrode collected current; L (1440 μm) and W (50 μm) are the channel length and width, respectively; μ is the mobility of the device; C_i (11 nF cm^{-2}) is the capacitance per unit area of the gate dielectric layer; V_{GS} is the gate voltage, V_{th} is the threshold voltage, the V_{th} of the device was determined by extrapolating the $(I_{DS},sat)^{1/2}$ vs. V_{GS} plot to $I_{DS} = 0$.

3. Synthesis

PNV: *N*-(2-octyldodceyl)-4,9-dibromonapthalene diimde (0.342 g, 0.33 mmol) and trans-1,2-bis(trimethylstannyl)ethene (0.200 g, 0.33 mmol) were dissolved in 12 mL toluene, stired and purged three times by vacuum/argon cycling. Then $Pd_2(dba)_3$ (12 mg, 2.0 mol%) and Tri(o-tolyl)phosphine (12 mg, 6 mol%) were added into the reaction mixture at liquid nitrogen bath and purged three times to remove oxygen of catalyst and ligands. The reaction solution was stirred at 120 ℃ for 3days. The crude product was poured into methanol. The precipitate was filtered. The solid was extracted by Soxhlet with acetone and hexane, finally the product was extracted with chloroform, and the chloroform was then removed under reduced pressure provided dark red solid (240 mg, 81.1%). ^1H NMR (600 MHz, $CDCl_3$): 1H NMR (600 MHz, CDCl3) δ 9.24 (2H, br), 8.97 (2H, br), 4.21 (4H, br) , 2.09 (2H, br), 1.29-1.20 (64H, m), 0.83 (12H, br);

Elementry analysis: calcd. for $C_{56}H_{88}N_2O_5$ (%): C, 77.37; H, 10.20; N, 3.22; found: C, 76.67; H, 10.10; N, 3.16.

4. TGA analysis

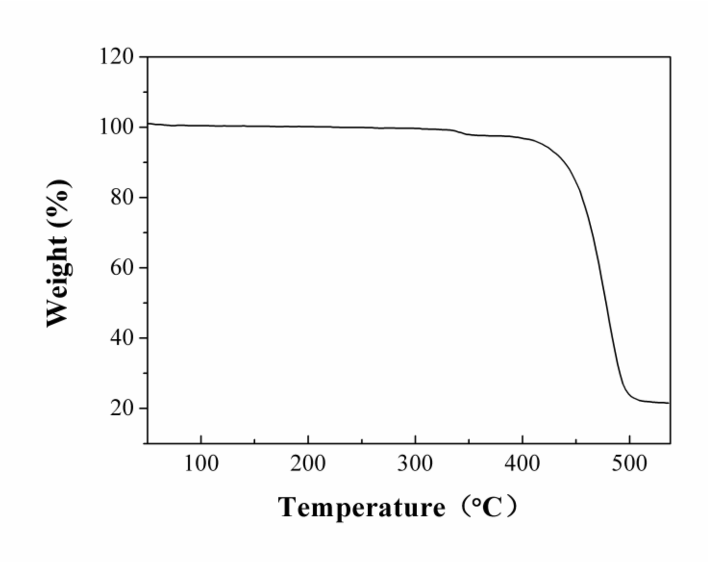

Figure S1. TGA analysis of PNV, T_d = 443 °C.

5. Circle voltammetry

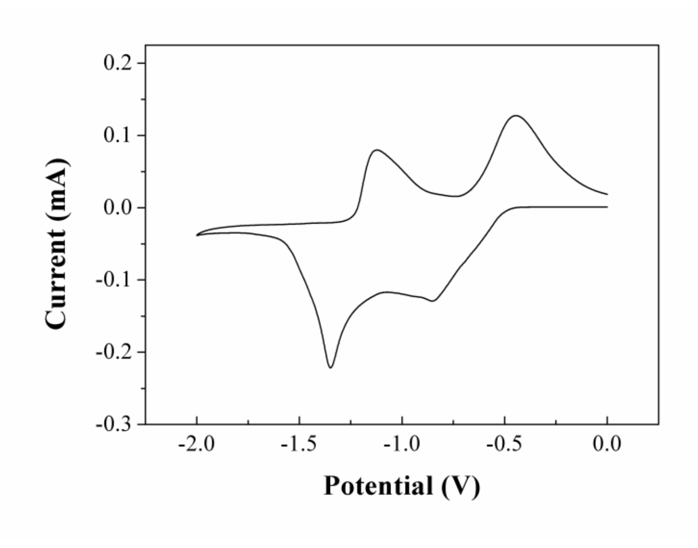

Figure S2. cyclic voltammetry of PNV in drop casted thin films.

6. Fluorescence lifetime measurement

Time-resolved emission-decay behaviors of PNV in both solution and thin films are measured with the excitation wavelength under 470 nm, of which the absorption is around 0.02 in thin film and 0.03 in solution (2 $\times 10^{-6}$ M, $CHCl_3$). The lifetime data were processed according to the literature method.[1] In solution of PNV the decay in the fluorescence intensity exhibit a single-exponential method while in thin film the decay in fluorescence was fitted by a double-exponential function. The results were summarized in the following Table S1.

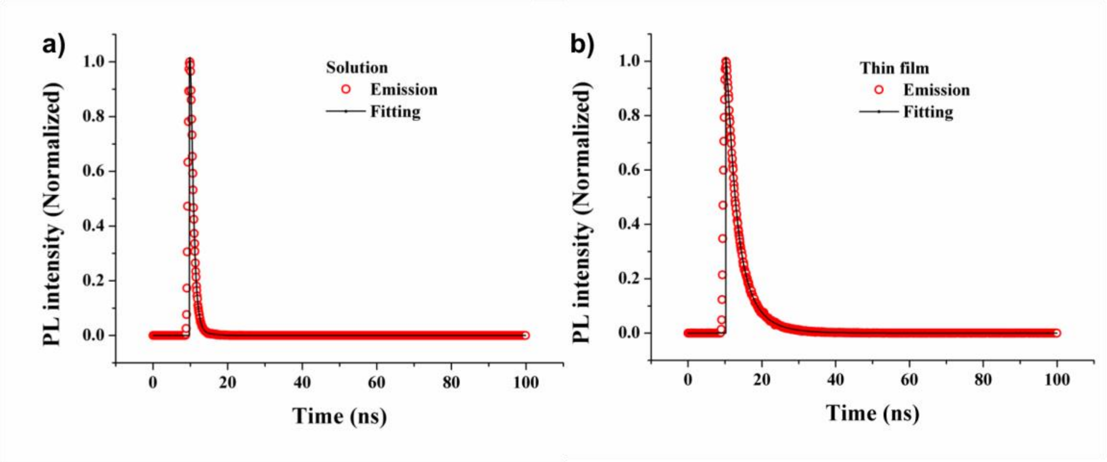

Figure S3. Time-resolved emission-decay curves of PNV in solution (a) and film (b).

Table S1. Fluorescence decay parameters of PNV in solution and thin film.

PNV	τ_1 (ns)	A_1	τ_1 (ns)	A_2	<τ> (ns)
Solution	0.60	0.26	/	/	0.60
Film	2.18	0.11	5.44	0.038	3.67

7. Excitation spectra

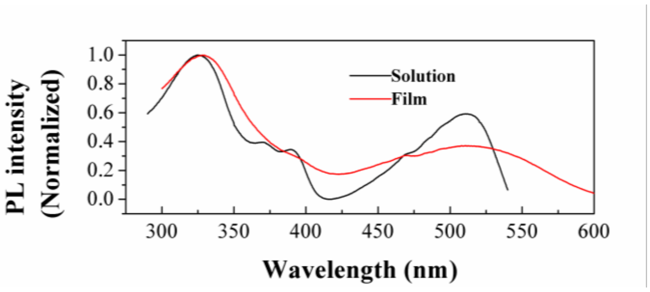

Figure S4. Excitation spectra for PNV in solution ($CHCl_3$, 10^{-5} M) and thin film.

8. DFT calculation

The energy of the complete co-planar conformation of PNV oligomer (n=2) has also been calculated. The results manifest an energy difference of 2.38 kcal/mol between the slight twisted conformation (energy = -2129.200642 hartree) we presented in the main paragraph and the complete co-planar conformation (energy = -2129.196868 hartree). According to Boltzmann distribution, the ratio of the two conformation is estimated to be 98.2/1.8, which indicates the slight twisted conformation hold much greater majority. A rigid potential energy scan of the bond angles around the NDI-vinylene is also presented as follow.

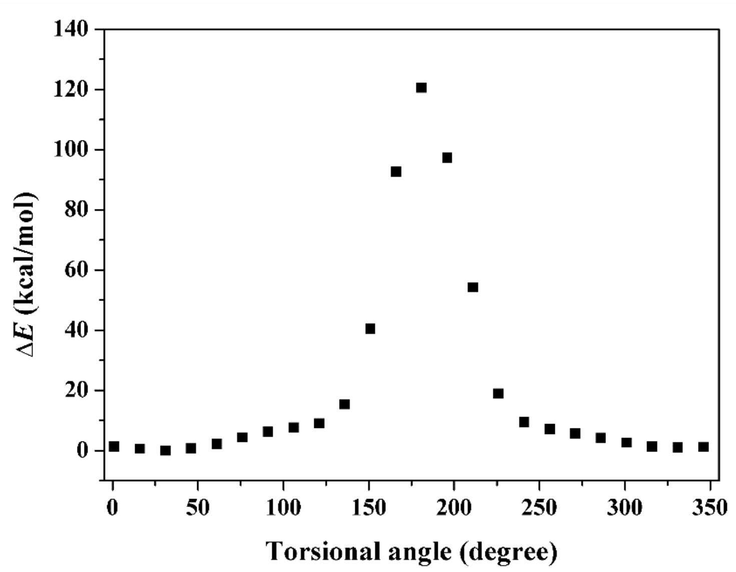

Figure S5. Rigid potential energy scan of the bond angles around the NDI-vinylene

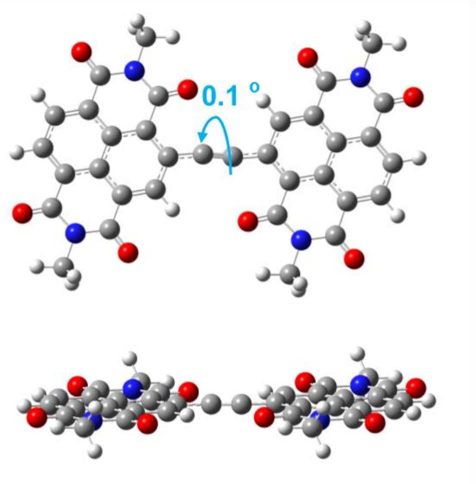

Figure S6. Front and side view of alkyne-linked NDI oligomer (n=2).

The DFT calculation on alkyne-linked NDI oligomer (n=2) revealed that the triple-bond link resulted in a more planar polymer backbone as depicted in Figure S5. The twist angle from the alkyne to NDI planar was only 0.1°. The calculated coordinates of PNV oligomer (n = 2) and alkyne-linked NDI oligomer (n=2) were listed as follow, respectively.

PNV oligomer

C	6.981398	0.527141	-0.057
C	6.5162	1.849271	-0.04146
C	5.159112	2.122845	0.000733
C	4.212017	1.069829	0.031607
C	4.693585	-0.26714	0.018611
C	6.081188	-0.52346	-0.02686
C	2.813881	1.327229	0.077347
C	1.902381	0.257204	0.131613
C	2.416091	-1.06939	0.120639
C	3.763459	-1.33081	0.057539
C	4.24018	-2.74158	0.052603
N	5.625512	-2.9422	-0.00012
C	6.589514	-1.92287	-0.04064
C	4.717092	3.538876	0.015989
N	3.333463	3.748405	0.029058
C	2.356011	2.743067	0.017324
O	7.778178	-2.17598	-0.08401
O	3.481581	-3.6906	0.088574
O	1.182119	3.069517	-0.04328
O	5.503298	4.467731	0.011028
C	6.079352	-4.34097	-0.00918
C	2.835299	5.132609	0.003055
C	0.449349	0.437938	0.244556
C	-0.44936	-0.43784	-0.2445
C	-1.90239	-0.25714	-0.13154
C	-2.41613	1.069443	-0.12044
C	-3.7635	1.330828	-0.05733
C	-4.69361	0.26713	-0.01854
C	-4.21201	-1.06983	-0.03172
C	-2.81387	-1.32719	-0.07741
C	-6.08121	0.523407	0.026994

C	-6.9814	-0.52722	0.056975
C	-6.51617	-1.84934	0.041149
C	-5.15907	-2.12287	-0.00108
C	-4.717	-3.53889	-0.01668
N	-3.33337	-3.74838	-0.02952
C	-2.35595	-2.74301	-0.01744
C	-4.24026	2.74158	-0.05219
N	-5.62561	2.942158	0.000324
C	-6.58957	1.922806	0.041074
O	-1.18206	-3.0694	0.043408
O	-5.50319	-4.46776	-0.01214
O	-3.48168	3.690626	-0.08782
O	-7.77823	2.175887	0.084823
C	-2.83518	-5.13258	-0.00373
C	-6.07947	4.340916	0.00957
H	8.04114	0.308826	-0.09185
H	7.20841	2.681604	-0.06146
H	1.73574	-1.90844	0.194327
H	7.163939	-4.33967	-0.04839
H	5.729485	-4.84643	0.891034
H	5.665668	-4.85579	-0.87647
H	2.170901	5.298527	0.850523
H	3.693869	5.794423	0.053484
H	2.272601	5.306727	-0.91442
H	0.115337	1.329497	0.754405
H	-0.11533	-1.32939	-0.75435
H	-1.73579	1.908513	-0.19402
H	-8.04114	-0.30894	0.091917
H	-7.20836	-2.68169	0.060946
H	-2.17029	-5.29815	-0.85087
H	-2.27302	-5.30703	0.914023
H	-3.6937	-5.7944	-0.05488
H	-7.16414	4.339575	0.046342
H	-5.66788	4.855079	0.878274
H	-5.72744	4.847082	-0.88938

Alkyne-linked NDI oligomer

C	7.025897	-0.86049	0.0096
C	6.434629	-2.13246	-0.00366
C	5.057491	-2.27024	-0.01169
C	4.221033	-1.12778	-0.00664

C	4.827375	0.158541	0.006587
C	6.234042	0.27494	0.014685
C	2.808766	-1.25263	-0.01378
C	2.012128	-0.09662	-0.00763
C	2.638048	1.184053	0.004244
C	4.005917	1.310705	0.011469
C	4.620491	2.667096	0.025054
N	6.02005	2.727728	0.033619
C	6.878938	1.617279	0.029064
C	4.465877	-3.63074	-0.02547
N	3.071435	-3.70753	-0.03301
C	2.192338	-2.60912	-0.0276
O	8.087509	1.750366	0.036658
O	3.959133	3.686574	0.029108
O	0.988929	-2.78126	-0.03428
O	5.143137	-4.64223	-0.03029
C	6.6112	4.074376	0.048194
C	2.497904	-5.06239	-0.04727
C	0.597044	-0.0982	-0.01089
C	-0.597	0.098567	-0.01083
C	-2.01209	0.096862	-0.00756
C	-2.63788	-1.18388	0.004322
C	-4.00574	-1.31067	0.011532
C	-4.82731	-0.15858	0.006614
C	-4.2211	1.127796	-0.00659
C	-2.80884	1.252788	-0.01373
C	-6.23397	-0.27512	0.014705
C	-7.02593	0.860228	0.009619
C	-6.43479	2.132253	-0.00363
C	-5.05767	2.270175	-0.01167
C	-4.46619	3.630737	-0.02545
N	-3.07176	3.707665	-0.0332
C	-2.19255	2.609343	-0.0275
C	-4.62018	-2.66712	0.025101
N	-6.01973	-2.72789	0.033536
C	-6.87873	-1.61753	0.029037
O	-0.98916	2.781619	-0.03398
O	-5.14355	4.642159	-0.03016
O	-3.95872	-3.68653	0.029219
O	-8.08729	-1.75073	0.036658
C	-2.49837	5.062583	-0.04754
C	-6.61075	-4.0746	0.048041
H	8.102516	-0.74668	0.016027

H	7.043268	-3.028	-0.00775
H	2.016569	2.070806	0.007966
H	7.690928	3.964997	0.05639
H	6.289417	4.626484	-0.83498
H	6.274374	4.6135	0.933723
H	1.416968	-4.96974	-0.05437
H	2.842436	-5.59612	-0.93309
H	2.82931	-5.6096	0.835387
H	-2.01632	-2.07057	0.008063
H	-8.10254	0.746312	0.016043
H	-7.04352	3.027736	-0.00773
H	-1.41743	4.970037	-0.05549
H	-2.84367	5.59648	-0.93296
H	-2.82911	5.60956	0.835516
H	-7.69049	-3.96533	0.055956
H	-6.28866	-4.62672	-0.83501
H	-6.27411	-4.61364	0.933696

9. ^{1}H NMR

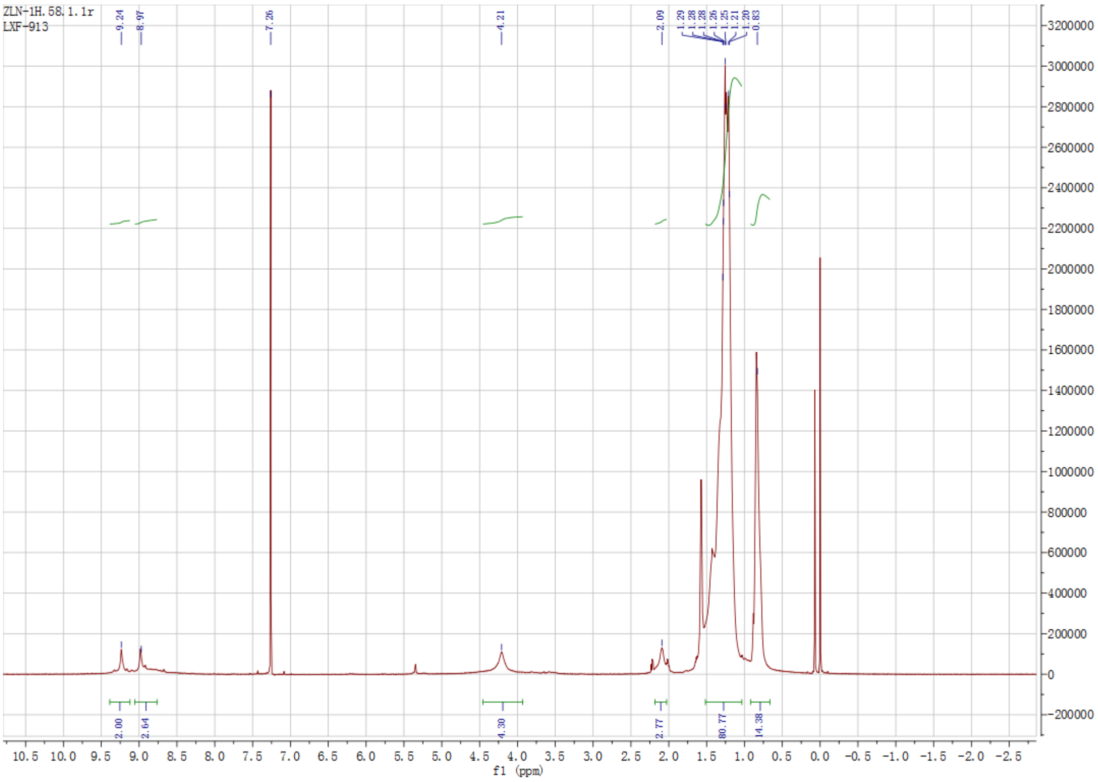

Figure S7. ^{1}H NMR spectrum of PNV (600 MHz, CDCl$_3$).

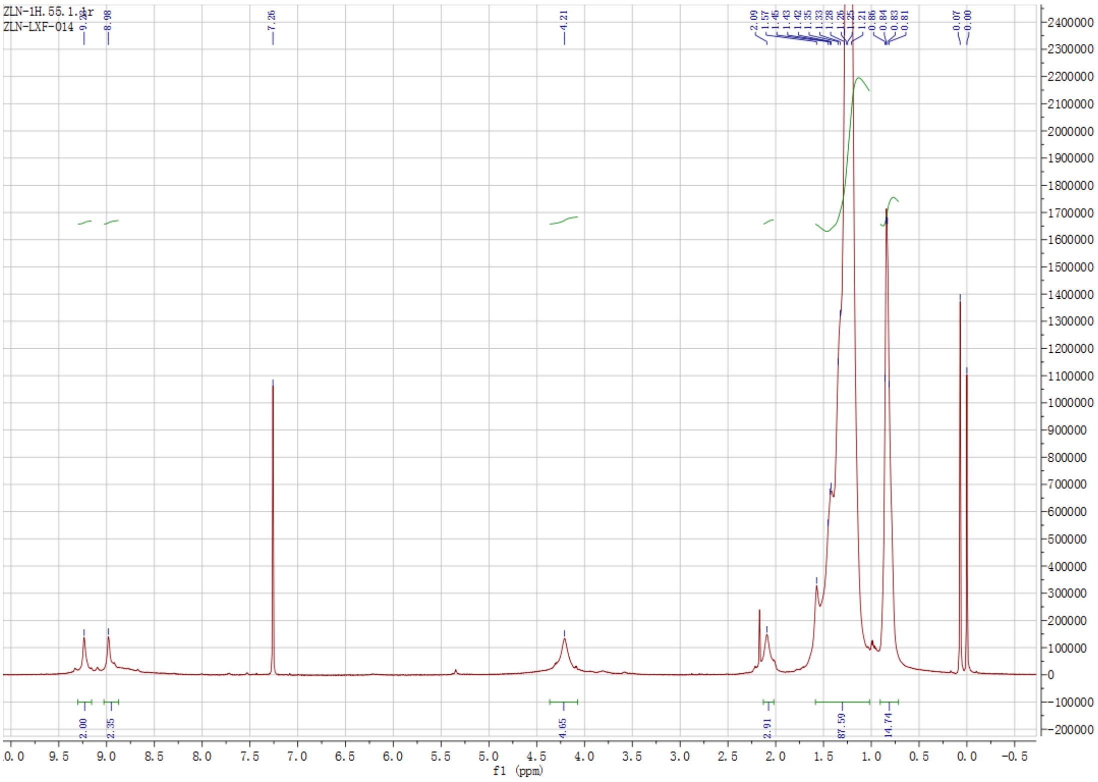

Figure S8. ^{1}H NMR spectrum of the second batch PNV (600 MHz, CDCl$_3$).

10. C-H…O bond evidence

A variable-temperature ^{1}H NMR for PNV in $C_2D_2Cl_4$ solvent from 298 K to 373 K has been performed. The results are as displayed in Figure S9, as depicted the corresponding proton peak of vinyl exhibits a slight shift to high field along the rising temperature, which is a typical effect from the disruption of hydrogen bonds.

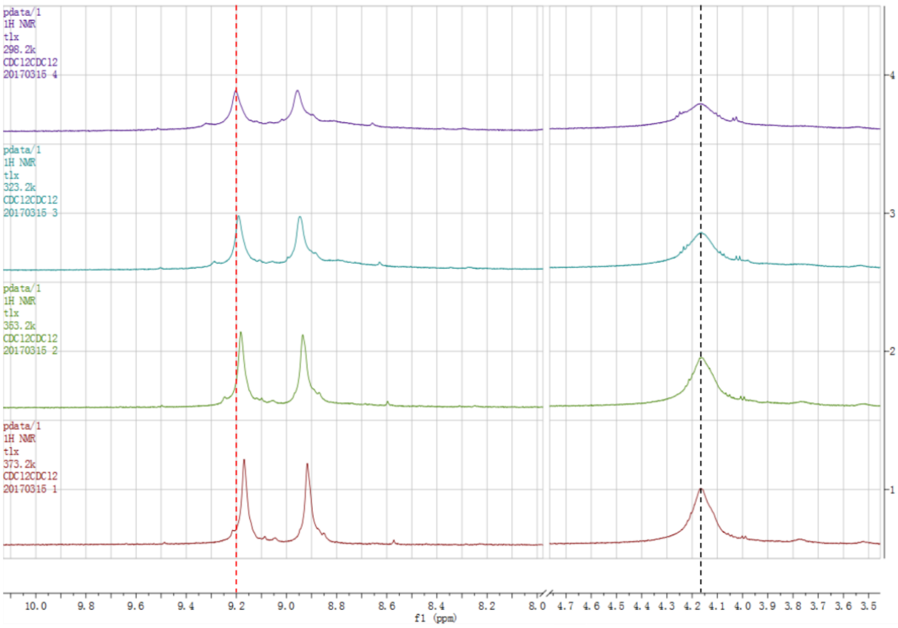

Figure S9. Variable-temperature ^{1}H NMR spectra for PNV in $C_2D_2Cl_4$ solvent.

The IR spectroscopy (Figure S10) was carried out for further proof on the H bond. A NDI-ethynylene copolymer was synthesized as a comparative compound. Out-of-plane vinyl C−H bending is known to give strong IR absorptions for both *cis* (600−700 cm^{-1}) and *trans* (900−1000 cm^{-1}) stereoisomers.[2] In PNV it should have the equal intensity as the Ar-H bending peak from the NDI core (800 cm^{-1}, as marked in figure S10). However, such bending vibration peak of vinyl (around 970 cm^{-1}) is obviously suppressed in PNV compared with the neighboring Ar-H bending peak and the one reported in poly(thiophene) vinylene.[3] This indicates a restriction effect on such vibration, which is possibly due to the H bond binding. On the other hand, the stretching vibration of 'C=C-H' in PNV blue shifted to 3110 cm^{-1} compared with PPV (3026 cm^{-1}) and dibutyl fumarate (3068 cm^{-1}, from Chemistry Database, CAS), which is also considered as a side proof of C-H…O bond.[4]

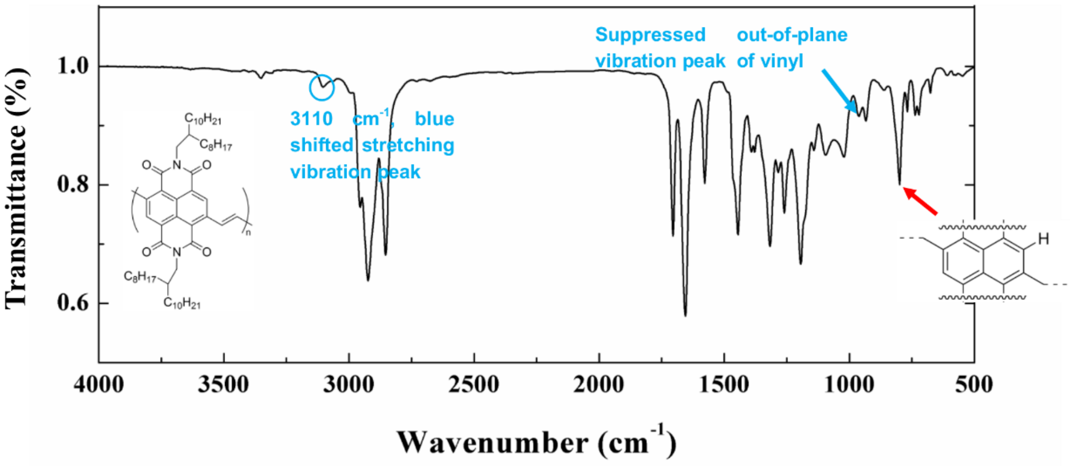

Figure S10. IR spectra of PNV.

Both the UV-Vis absorption variation and fluorescence spectra of PNV in the chloroform/anisole combination have been measured for further supporting of the existence on H bond. For UV-Vis absorption, to avoid interference of anisole's absorption, the spectra were obtained above 350 nm. The main absorption peak at 516 nm obviously decreases as the volume fraction of anisole increases. For fluorescence, the emission at 550 nm gradually decreases to 15% of its original intensity with no further emerging of emission around 620 nm as in chloroform/hexane combination. These results support the fact that the H-bonding is possibly disrupted by the addition of anisole.

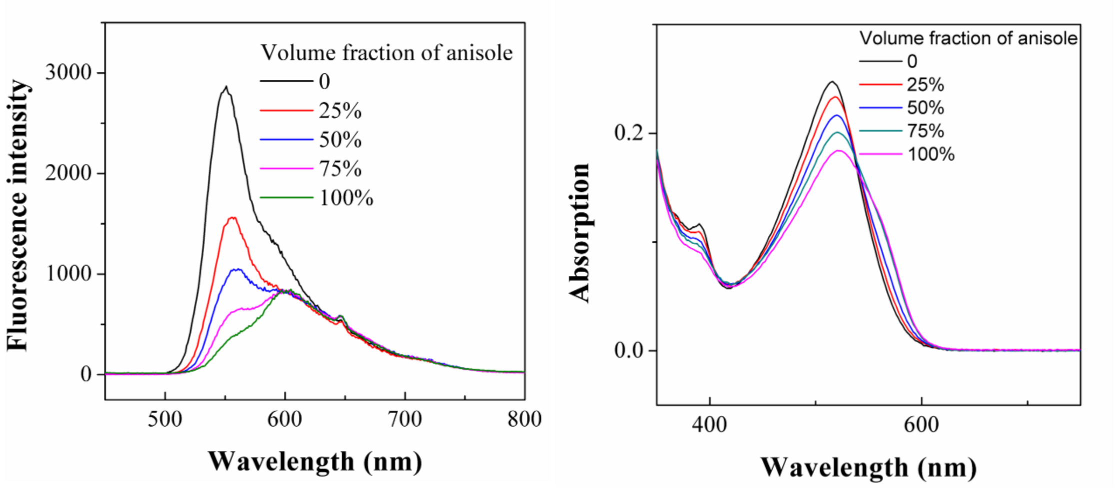

Figure S11. Fluorescence (left) and UV-Vis (right) absorption spectra variation of PNV in chloroform/anisole solution (10^{-5} M)

11. References

1. A. Qin, C. K. Jim, Y. Tang, J. W. Y. Lam, J. Liu, F. Mahtab, P. Gao and B. Z. Tang, *J. Phys. Chem. B* 2008, **112**, 9281.

2. E. Pretsch, P. Bühlmann, C. Affolter, *Structure Determination of Organic Compounds: Tables of Spectral Data*, Springer: Heidelberg, Germany, 2000, p248.

3. J. C. Speros, H. Martinez, B. D. Paulsen, S. P. White, A. D. Bonifas, P. C. Goff, C. D. Frisbie and M. A. Hillmyer, *Macromolecules* 2013, **46**, 5184.

4. P. Hobza and Z. Havlas, *Chem. Rev.* 2000, **100**, 4253.